291

N94-12307

Superfluid turbulence

By D. C. Samuels

1. Motivation and objectives

At low temperatures (below 5 Kelvin), helium is a liquid with a very low kinematic viscosity. It has been proposed (Liepmann and Coles (1979), Donnelly (1991)) that wind tunnels could be built using liquid helium as the test fluid. The primary advantages of such wind tunnels would be a combination of large Reynolds numbers and a relatively small apparatus. It is hoped that this combination will allow the study of high Reynolds number flows in an academic setting.

There are two basic types of liquid helium wind tunnels that can be built, corresponding to the two phases of liquid helium. The high temperature phase (between approximately 2 to 5 Kelvin) is called helium I and is a Navier-Stokes fluid. There are no unanswered scientific questions about the design or operation of a wind tunnel in the helium I phase.

The low temperature phase (below approximately 2 Kelvin) of liquid helium is called helium II. This is a *quantum fluid*, meaning that there are some properties of helium II which are directly due to quantum mechanical effects and which are not observed in Navier-Stokes fluids. The quantum effects that are relevant to this paper are:

(1) Helium II is well described as a superposition of two separate fluids called the *superfluid* and the *normal fluid*. The normal-fluid component is a Navier-Stokes fluid and the superfluid is an irrotational Euler fluid.

(2) Circulation in the superfluid exists only in quantized vortex filaments. All quantized vortex filaments have identical circulations κ and core size a.

One would expect that with these quantum effects the flow of helium II would show departures from Navier-Stokes behavior. Indeed, helium II flows with thermal gradients do not show classical Navier-Stokes behavior. This type of helium II flow has been the most widely studied precisely due to its unusual properties. Recently, isothermal flows have been examined in numerous experiments (see Walstrom *et al.* (1988) and Borner *et al.* (1983) for example). The surprising result of these experiments is that the isothermal flow of helium II appears to behave as a Navier-Stokes fluid. It has been consistently observed in a wide range of flow geometries that the measurable parameters of the flow obey the same laws (empirical and theoretical) as Navier-Stokes fluids. For a description of some of these experiments, see Donnelly (1991).

This apparent Navier-Stokes behavior of isothermal helium II flows could be exploited to study turbulence with a helium II wind tunnel. Some advantages of a

helium II wind tunnel over the helium I wind tunnel are listed by Donnelly (1991) and I will not repeat them here except to say that the technology exists to directly observe vorticity in helium II. This measurement is made possible through the attenuation of *second sound*, a type of sound which only exists in superfluids, by the quantized vortex filaments in the superfluid component. This is a basic technique very commonly used in helium II experiments.

The objective of my research at CTR has been to develop an understanding of the microscopic processes responsible for the observed Navier-Stokes behavior of helium II flows.

2. Accomplishments

The simplest interpretation of the experimental data on helium II flow is that the normal fluid is somehow entraining the superfluid so that both components have the same, Navier-Stokes flow behavior. Since the superfluid can only contain circulation in the form of quantized vortex filaments, it is natural to suspect that the interaction of these quantized vortex filaments with the normal-fluid flow is somehow the cause of the superfluid entrainment. I investigated the vortex filament behavior by simulations of the filament motion in a spatially non-uniform flow field of the normal-fluid. The vortex filaments are represented in the simulations by a series of mesh points placed along the filament. The equation of motion of each mesh point is

$$\frac{d\mathbf{X}}{dt} = \mathbf{v_s} + \mathbf{v_v} + \alpha \mathbf{t} \times (\mathbf{v_n} - (\mathbf{v_s} + \mathbf{v_v})), \tag{1}$$

where $\mathbf{X}$ is the position of the point on the vortex filament, $\mathbf{v_s}$ is the irrotational part of the superfluid velocity field, $\mathbf{v_v}$ is the local velocity due to all the vortex filaments in the fluid, α is a temperature dependent coefficient, $\mathbf{t}$ is the local unit tangent vector of the filament, and $\mathbf{v_n}$ is the local velocity of the normal fluid. The first two terms on the right hand side of equation 1 are simply the total local superfluid velocity. The third term describes the response of the vortex filament to the normal-fluid velocity $\mathbf{v_n}$ due to the scattering of the normal fluid by the vortex filament. This process is called *mutual friction* and is well understood from first principles (Samuels and Donnelly (1990)). The numerical methods used to integrate equation 1 and to form and update the meshing of the vortex filaments are described in Samuels (1991) and Samuels (1992a).

2.1 Laminar flows

Though the final goal is to gain an understanding of the superfluid entrainment process in turbulent flows, I began this project with simulations of Poiseuille flow of helium. There was some indication in the experiments that the superfluid entrainment was not limited to high Reynolds number flows, but may also occur in low speed, laminar flows (Murakami and Ichikawa (1989)). The experimental evidence for this is small simply because there were very few experiments actually done in the low Reynolds number range due to the very low flow speed required for the laminar flow of helium II. If laminar flows did show superfluid entrainment, I expected that some basic understanding of the entrainment process could be more easily gained

in this simple flow. I would then attempt to apply this understanding to the more complex flows characteristic of turbulence.

From the results of my laminar flow simulations, I proposed two necessary conditions for the entrainment of the superfluid in a general flow. These conditions are:

(1) A region of locally matched velocity $v_n = v_s$ must initially exist in the flow.

(2) A source of quantized vortex filament must be present.

Through the mutual friction term in the equation of motion (equation 1), vortex filaments will move toward the region of locally matched velocity (called the nodal surface). The effect of the mutual friction is to hold and orient the vortex filaments at the nodal surface so that the circulation of the vortex filament is in the same direction as the local circulation of the normal fluid. As more filaments accrete onto the nodal surface (hence the need for condition 2), the filament density increases until the superfluid circulation, averaged over a region containing many filaments, equals the local normal-fluid circulation. Filaments that are too far apart will be moved closer together by mutual friction and filaments that are too close will be pushed farther apart. The stable point is where the local superfluid and normal-fluid velocity fields are equal, which makes the mutual friction term in the equation of motion equal to zero. The result of this process is that an ordered array of quantized vortex filaments forms around the nodal surface with sufficient density to equal the local circulation density in the normal fluid, thus entraining the superfluid to the normal fluid.

A simple example of the entrainment of the superfluid by the normal fluid is given in figure 1. In this example, I am considering the flow of helium II through a circular pipe. Figure 1a shows the initial velocity profiles of both the superfluid and the normal fluid. The normal fluid has a parabolic profile with zero velocity at the pipe wall. The superfluid, with no initial vortex filaments, has a flat velocity profile that slips completely at the pipe walls. The magnitude of the superfluid velocity is set to be equal to the average normal-fluid velocity. Though the flow rates of the two fluids are equal, the local velocities are only equal at a specific radius inside the pipe. This radius marks the nodal surface (condition 1 above) for this geometry.

As the quantized vortex filaments are generated by the velocity difference at the pipe wall (a process described in detail in Samuels (1992a)), they gather in an ordered manner about the nodal surface. The combined velocity fields of all the vortex filaments produce an approximately parabolic velocity profile in the superfluid that matches the local velocity profile of the normal fluid (figure 1b).

2.2 A simple model of turbulent flows

With the experience gained from the laminar simulations, the problem of superfluid entrainment in turbulent flows is reduced to a question of identifying the nodal surfaces and the process responsible for quantized vortex filament formation in a turbulent flow. For a simple model of turbulence, I chose an isolated, concentrated
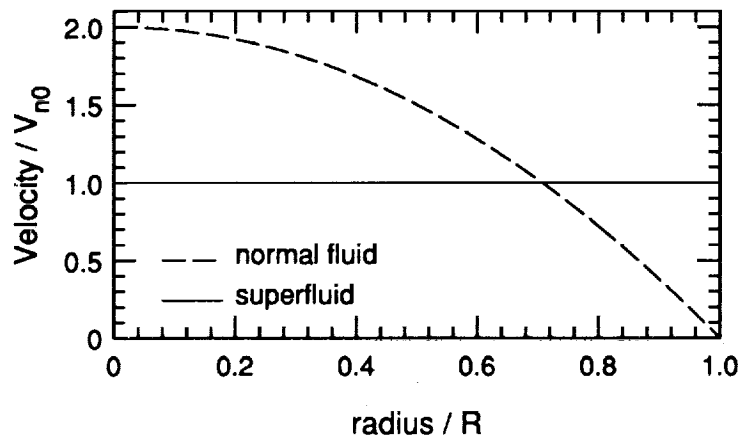
FIGURE 1A.   Initial velocity profiles of the normal fluid and superfluid in laminar pipe flow. R denotes the pipe radius. V_{n0} denotes the average normal fluid flow rate. The nodal surface is at a radius of $.707R$.
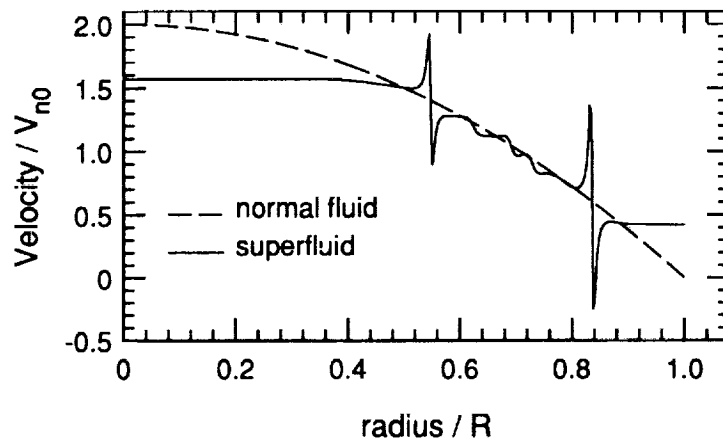

FIGURE 1B.   Normal fluid and superfluid velocity profiles after the formation of quantized vortex filaments.

vortex in the normal fluid. This is meant to represent the vortex tubes reported in experiments (Douady *et al.* (1991)) and simulations (Siggia (1981), Kerr (1985), Ruetsch and Maxey (1991)) of Navier-Stokes turbulence. I assume that the superfluid is initially at rest. With these initial conditions, there is a nodal surface on the axis of the normal-fluid vortex tube where both the superfluid and normal-fluid velocities are zero.

With the nodal surface identified, we must now find a process that will form large amounts of quantized vortex filaments. In the simulations reported in this paper, the normal-fluid vortex tube was represented by a gaussian distribution of circulation with the vorticity vector aligned along the Z axis. The core size of the vortex tube is denoted by r_c. In order to make the calculation spatially finite, the vortex tube was limited to a length of $20r_c$. This was accomplished by rapidly expanding the vortex-tube core size beyond this length. The geometry of the vortex-tube core is outlined by the dashed line in figure 2a. None of the results presented here were dependent on the length of the vortex tube as long as the length was greater than approximately $10r_c$. I typically used normal-fluid vortex tubes with circulations much greater than the small circulation of the quantized vortex filaments, so many vortex filaments must be formed to equal the normal-fluid circulation.

Figure 2 illustrates the process responsible for the formation of the vortex filaments. The simulation begins with a small vortex filament ring near the normal-fluid vortex tube (figure 2a). The vortex ring is aimed so that it moves toward the normal-fluid vortex tube under its own self-induced velocity. When the vortex ring reaches the normal-fluid vortex tube, it is captured on the center of the vortex tube (at the nodal surface) by mutual friction (figure 2b). It is then stretched along the vortex tube axis (again by mutual friction). As the vortex filament ring is stretched, it also twists around the vortex tube axis under its self-induced velocity (figure 2c). This three-dimensional twisting motion causes a section of the vortex filament ring to turn towards the azimuthal direction of the normal-fluid vortex core. At this section of the quantized vortex filament, there is now a normal-fluid velocity component (from the vortex tube) along the axis of the vortex filament. A quantized vortex filament with an axial normal-fluid flow is known to be unstable to the growth of a helical wave on the vortex filament (Ostermeier and Glaberson (1975)). Since the unstable length of the vortex filament is small in this situation, the instability to helical wave growth typically leads to the growth of a single loop (figure 2d) on the vortex filament, though I have seen situations where multiple loops are formed simultaneously. This new loop of quantized vortex filament is itself captured by the core of the normal-fluid vortex tube and will follow the same evolution as the initial vortex ring. Meanwhile, the initial vortex ring is still unstable and will continue forming new vortex loops until it eventually moves off the lower end of the vortex tube. This process of loop formation leads to an exponential growth in the length of quantized vortex filament. Figure 2e shows a later stage of this growth. By this time, a dense grouping of highly ordered quantized vortex filaments has formed within the normal-fluid vortex tube. To summarize, a concentration of vorticity in the normal fluid will form a corresponding concentration of
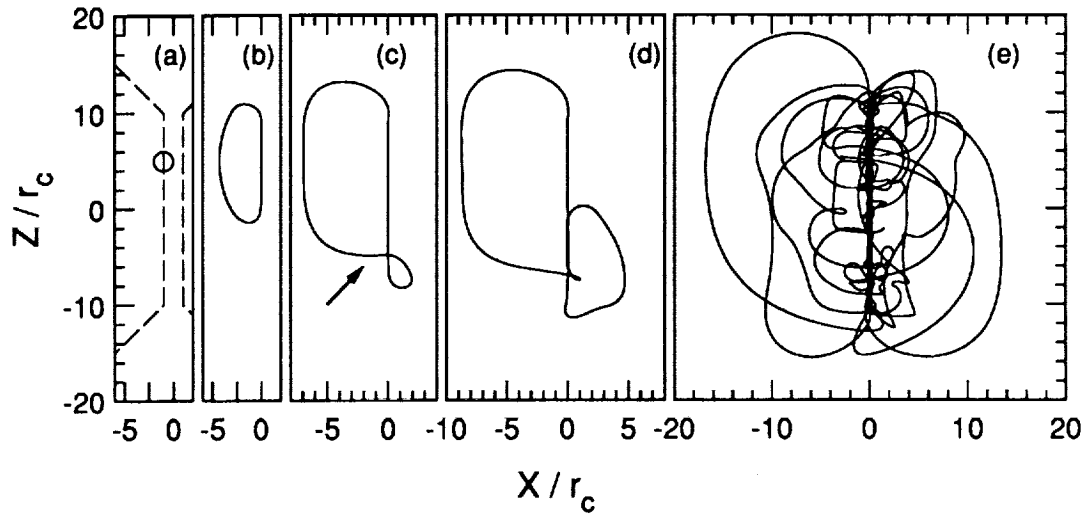
FIGURE 2. Evolution of the quantized vortex filament. Z denotes the direction along the axis of the normal-fluid vortex tube and X denotes the distance along one axis perpendicular to the vortex-tube axis. (a) Initial state. The solid lines denote the quantized vortex filament. Dashed lines outline the core of the normal-fluid vortex tube. (b) The quantized vortex filament is captured by the vortex tube. (c) Instability begins at the section of vortex filament marked by the arrow. (d) A new loop forms. (e) Quantized vortex filaments are concentrated in the core of the normal-fluid vortex tube.

quantized vortex filaments in the superfluid.

Figure 3 shows the velocity profile of the superfluid and the normal fluid along a line in the plane of the normal-fluid vortex tube and through its axis. At this point in the simulation, the quantized vortex filament was still growing (see figure 4), but the computation time per timestep had grown too large to continue the simulation. It is not yet known when this growth will eventually stop. Figure 4 shows the growth of the superfluid circulation within the core of the normal-fluid vortex tube. As expected, the growth is exponential. By the end of the simulation, the superfluid circulation had grown to approximately 35% of the normal-fluid circulation and was still growing exponentially.

From a large number of these simulations, I developed an empirical equation for the time constant τ of the exponential growth of the superfluid circulation Γ_c. This equation is

$$\tau = \frac{Cr_c^2}{\sqrt{\alpha}\Gamma_n} \tag{2}$$

where r_c is the core radius of the vortex tube, Γ_n is the circulation of the vortex tube, α is the mutual friction parameter from equation 1, and C is a dimensionless
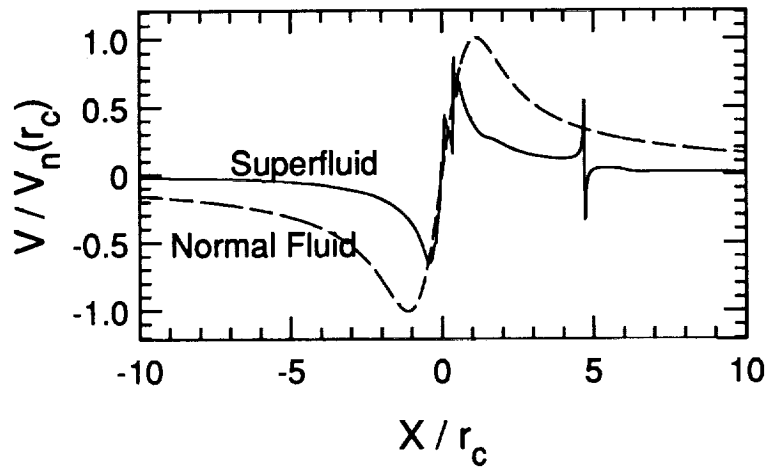
FIGURE 3. Superfluid and normal-fluid velocity profiles in the plane of the vortex tube. Velocities are normalized by the velocity at the core radius $V_n(r_c)$ and position X is normalized by the vortex-tube radius. The position is taken along an axis perpendicular to the vortex-tube axis.
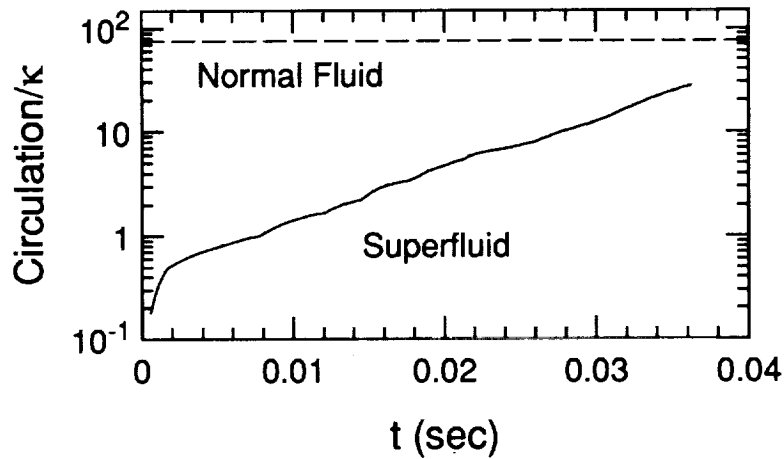

FIGURE 4. Exponential growth of the superfluid circulation inside the core of the normal-fluid vortex tube. The dashed line denotes the circulation of the vortex tube.

constant determined by least squares fit to be $C = 458 \pm 5$.

This process of superfluid filament growth is only useful if the time scale τ is small compared to the lifetime of the concentrated vortex tubes present in the turbulent normal fluid. To make this comparison, we must know the lifetime, core size, and circulation of typical vortex tubes in Navier-Stokes turbulence. These values are not well known at the current time. We take the lifetime to be one large eddy turnover time (Douady et al. (1991), the core radius to be $r_c \approx 3\eta$ where η is the Kolmogorov length scale (Ruetsch and Maxey (1991), Vincent and Meneguzzi (1991)), and the circulation to be $\Gamma_n = (300 \pm 100)\nu$ (Jimenez (1992)) where ν is the kinematic viscosity of the normal fluid. All of these values are taken from fairly low Reynolds number experiments or simulations and may very well change with future research. With this caveat, the ratio of the vortex tube lifetime t_{life} to the growth time scale τ is

$$\frac{t_{life}}{\tau} \simeq (.23 \pm .08)\sqrt{\alpha Re}, \tag{3}$$

where I have defined a Reynolds number $Re = U_I L_I / \nu_n$ with the large eddy velocity scale U_I and length scale L_I, and ν_n is the kinematic viscosity of the normal fluid. The mutual friction parameter α has a typical value of $\alpha = .1$, so for Reynolds numbers on the order of 1000 or higher, we expect the vortex tube lifetime to be large compared to the growth time constant τ. Therefore, in high Reynolds number flows the time required for the growth of the superfluid circulation should be small compared to the lifetime of the vortex tubes.

The growth process described above only occurs for normal-fluid vortex tubes with circulations stronger than a minimum value $\Gamma_{n,min}$. From least square fits of many simulations, this minimum value is found to be well described by the empirical formula

$$\frac{\Gamma_{n,min}}{\Gamma_s} = \frac{D}{\alpha} ln(\frac{r_c}{a}) - E, \tag{4}$$

where Γ_s is the circulation of the quantized vortex filaments, α is the temperature dependent mutual-friction parameter, a is the core size of the quantized vortex filaments, and D and E are constants fit from the simulation results. The values found for the constants are $D = 1.30 \pm .05$ and $E = 7.8 \pm .3$. This formula for $\Gamma_{n,min}$ should be compared to the observed circulations of vortex tubes in Navier-Stokes turbulence. From simulation results, Jimenez (1992) gives a value of

$$\Gamma_{tube} = Re_\gamma \nu \tag{5}$$

for the circulation of vortex tubes, where ν is the kinematic viscosity of the fluid and the circulation Reynolds number Re_γ is found to lie in the range $200 < Re_\gamma < 400$. As was stated before, this value for the vortex tube circulation was taken from low Reynolds number simulations and may change with higher Reynolds number. A comparison of $\Gamma_{n,min}$ and the range of vortex tube circulations from equation 5 is given in figure 5. Γ_{tube} has a temperature dependence (and hence an α dependence) through the kinematic viscosity of the normal fluid. For reasonable values of r_c, the minimum circulation $\Gamma_{n,min}$ lies within the range of expected vortex tube
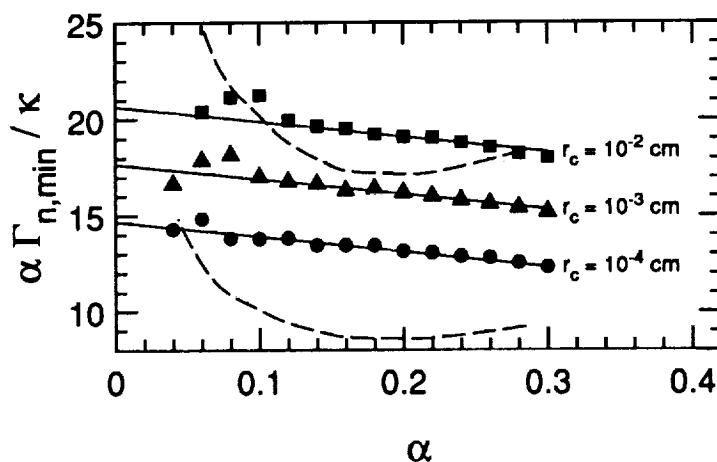
FIGURE 5.   Minimum circulation for the vortex filament instability *vs* α. The solid lines are from equation 5. The dashed lines outline the expected range of circulations of the normal-fluid vortex tubes.

circulations. The reader should remember that these simulations were done with a very simplified geometry, using a perfectly straight vortex tube with a uniform cross section. It is reasonable to expect that any nonuniformities in the vortex tube radius or direction would decrease the value of $\Gamma_{n,min}$ since they would act to locally increase the normal-fluid flow along the axis of the quantized vortex filament, which increases the instability of the filament. Thus, the values of $\Gamma_{n,min}$ given by equation 4 should be considered as upper bounds to the actual minimum unstable circulation. More details of these results are given in Samuels (1992b).

In summary, these simulations have identified a process which generates localized superfluid circulation inside the cores of the normal-fluid vortex tubes found in Navier-Stokes turbulence. This growth process is exponential with a time constant small compared to the vortex-tube lifetime taken from current turbulence research. The minimum circulation $\Gamma_{n,min}$ compares well with the vortex-tube circulations taken from Navier-Stokes turbulence simulations. It also should be pointed out that the dense array of quantized vortex filaments formed in the cores of the normal-fluid vortex tubes should allow the detection of these vortex tubes by the attenuation of second sound.

3. Future plans

Though the central objective of the research project has been met, there remain several unresolved issues. Primarily among these is the question of when the growth process shown in figure 4 stops. As stated earlier, the computation time necessary for such a large amount of vortex filament prevented me from running

the simulations to a final steady state. It is possible that simulations in a different parameter range will converge to a steady state within a reasonable computation time. Preliminary work on this approach has been promising.

Once a steady state configuration is available from the simulations, the response of this coupled normal fluid - superfluid state to external perturbations could be examined. This would be an important test of the approximation that the coupled state can be treated as a single component fluid obeying the Navier-Stokes equation.

The most difficult extension of this work would be to include a true interaction between the two fluids. The present simulations are done with an imposed normal-fluid velocity field which is constant in time. In reality, the normal fluid must respond to the motion of the superfluid. To directly include this interaction in the simulations would require an enormous increase in the complexity of the problem. We can say that the use of a non-reacting normal-fluid velocity field is likely to be a good approximation at higher temperatures (near 2 Kelvin) where the normal-fluid density is greater than the superfluid density.

REFERENCES

BORNER, H., SCHMELING, T., & SCHMIDT, D. W. 1983 Experiments on the circulation and propagation of large-scale vortex rings in He II. *Phys. Fluids.* **26**, 1410-1416.

DONNELLY, R. J. 1991 *High Reynolds Number Flows Using Liquid and Gaseous Helium.* Springer Verlag.

DOUADY, S., COUDER, Y., & BRACHET, M. E. 1991 Direct observation of the intermittency of intense vorticity filaments in turbulence. *Phys. Rev. Lett.* **67**, 983-986.

JIMENEZ, J. 1992 Kinematic alignment effects in turbulent flows. *Phys. Fluids A.* **4**, 652-654.

KERR, R. M. 1985 Higher-order derivative correlations and the alignment of small-scale structures in isotropic numerical turbulence. *J. Fluid Mech.* **153**, 31-58.

LIEPMANN, H. W. & COLES, D. 1979 *Proceedings of the Workshop on High-Reynolds-Number Flow.* California Institute of Technology.

MURAKAMI, M. & ICHIKAWA, N. 1989 Flow visualization study of thermal counterflow jet in He II. *Cryogenics.* **29**, 438-443.

OSTERMEIER, R. M. & GLABERSON, W. I. 1975 Instability of vortex lines in the presence of axial normal fluid flow. *J. Low Temp. Phys.* **21**, 191-196.

RUETSCH, G. R. & MAXEY, M. R. 1991 Small-scale features of vorticity and passive scalar fields in homogeneous isotropic turbulence. *Phys. Fluids A.* **3**, 1587-1597.

SAMUELS, D. C. & DONNELLY, R. J. 1990 Dynamics of the interactions of rotons with quantized vortices in helium II. *Phys. Rev. Lett.* **65**, 187-191.

SAMUELS, D. C. 1991 Velocity matching in superfluid helium. *CTR Annual Research Briefs* Stanford Univ./NASA Ames. **93-104.**

SAMUELS, D. C. 1992a Velocity matching and Poiseuille pipe flow of superfluid helium. *Phys. Rev. B.* **46,** 11714-11724.

SAMUELS, D. C. 1992b Response of superfluid Vortex filaments to concentrated normal fluid vorticity. *Phys. Rev. B, Brief Rep.,* to appear.

SIGGIA, E. D. 1981 Numerical study of small-scale intermittency in three-dimensional turbulence. *J. Fluid Mech.* **107,** 375-406.

VINCENT, A. & MENEGUZZI, M. 1991 The spatial structure and statistical properties of homogeneous turbulence. *J. Fluid Mech.* **225,** 1-20.

WALSTROM, P. L., WEISEND II, J. G., MADDOCKS, J. R., & VAN SCIVER, S. W. 1988 Turbulent flow pressure drop in various He II transfer system components. *Cryogenics.* **28,** 101-109.